



Article

Nanomechanical Properties of a Bicomponent Epoxy Resin via Blending with Polyaryletherketone

Haixia Hu ^{1,2,*}, Zhiwei Liu ^{1,2}, Chengjun Wang ^{1,2}, Limin Meng ^{1,2} and Yuzhe Shen ^{1,2}

¹ College of Mechanical Engineering, Anhui University of Science and Technology, Huainan 232001, China; lzwlws@aust.edu.cn (Z.L.); cjwang@aust.edu.cn (C.W.); lmmeng@aust.edu.cn (L.M.); yzshen@aust.edu.cn (Y.S.)

² Anhui Key Laboratory of Mine Intelligent Equipment and Technology, Anhui University of Science & Technology, Huainan 232001, China

* Correspondence: huhx@aust.edu.cn; Tel.: +86-554-666-8934

Received: 4 August 2019; Accepted: 17 September 2019; Published: 26 September 2019



Abstract: In order to investigate the nanomechanical behaviors and nanotribological properties of bicomponent epoxy resin (BE) blends, which were filled with thermoplastic polyaryletherketone (PAEK) powders, nanoindentation and nanoscratch tests were performed. The brittle fractured morphologies of bicomponent epoxy resin blends were studied. The microhardness and elastic modules of the materials were measured using the nanoindentation technology. The hardness, elastic modulus, and other mechanical properties of materials on a nanoscale were determined. Nanoindentation and scratch experiments showed that the indentation response is dominated by plastic deformation. The microhardness is the lowest as the content of PAEK powders is increased to 30 parts per hundred parts of resin (phr), while that of the neat bicomponent epoxy resin specimen is the highest. Furthermore, the pristine bicomponent epoxy resin (BE) exhibited better load-carrying and indentation recovery capacity than the other three samples. The nanoscratch results indicate that the frictional coefficient of the BE/PAEK-30 blend is the lowest, and while that of the pristine bicomponent epoxy resin is the highest, with better scratch/wear resistance.

Keywords: bicomponent epoxy resin; blends; nanomechanical properties; nanotribology

1. Introduction

With the development of precision and ultra-precision machining technology, many microstructures are applied in engineering practice. Therefore, the mechanical properties of materials at the nanoscale attracted great attention. In fact, the researches on microelectronics and micro-mechanical processing showed that the properties of materials at this scale are different from those of macroscopic materials. The properties of their surface and near-surface mechanical behaviors, such as hardness, elastic modulus, creep, and yield stress, were shown to govern the performance of such components. Therefore, recent advances in miniaturization of polymer components for nanotechnology applications require the characterization of their properties [1]. For this purpose, nanoindentation and nanoscratching technologies are widely used to probe the mechanical properties, deformation, and removal mechanisms involved in ultra-precision machining [2]. Nanoindentation is an important technique for probing the mechanical properties of engineering materials. Nanoindentation technology was widely used in the study of the nano-mechanical properties of materials in the past 10 years due to its lower invasiveness in a small local area [3]. These techniques can record load and depth continuously to evaluate the nanomechanical and tribological properties of a solid material based on the local deformation [4]. Generally speaking, the resistance to indentation of the composites gradually increases with the

increase in filler loading [1]. The hardness, elastic modulus, and other nanomechanical properties of the materials on a nanoscale were measured using nanoindentation through measuring the applied load and indentation depth under an indenter tip [5]. This is a response to the occurrence of shear localization, cracking, or creeping [6]. Nanoscratch technology is an important area of research in the field of materials science and mechanics [7]. Scratching is a part of tribology. Clearly, a wide range of surface damage phenomena can be observed during scratching of polymers, making it a major obstacle in the fundamental understanding and prediction of scratch-induced damage in polymers.

Nanoscratch was extensively used to evaluate the friction and wear behaviors of polymers, as well as the material removal mechanisms, including plastic deformation, microstructure, and surface deformation mechanisms of materials or machine parts in material engineering and many industrial applications [8–11]. For some simple polymers, such as epoxy resins, polycarbonate, and poly (methyl methacrylate), nanoscale scratching results indicated that the surface damage encountered is material-specific [8].

Epoxy resin is an important thermosetting material with epoxy groups, increasingly used as a matrix resin for advanced fiber-reinforced composites in the aerospace, automobile, and marine industries, due to its excellent mechanical properties, corrosion resistance, chemical stability, and electrical and thermal conductivities [12]. Diaminodiphenylmethane tetraglycidyl epoxy resin (TGDDM) is widely used as a matrix resin for advanced fiber-reinforced composites in the aerospace and aircraft industries [13]. Due to the high three-dimensional cross-linked structure of cured epoxy resin, however, the brittleness is very high. Therefore, these materials have some undesirable properties such as low toughness and poor crack resistance and growth as a structural part, which constrain their applications. In order to meet further requirements, the two epoxy resins mentioned above were prepared into a new blend system (BE), which can provide a series of excellent mechanical properties, such as high strength, hardness, modulus, and fracture toughness [14]. In addition, in recent years, many studies were carried out to toughen the brittle thermosetting epoxy resins (TS) with engineering thermoplastics (TPs) [15,16]. Thermoplastic resins with high heat resistance and good mechanical properties served as toughening agents for modifying brittle epoxy resins for more than 30 years. The thermoplastic toughening can significantly improve the toughness of epoxy resins without decreasing its thermal mechanical properties [17]. Polyaryletherketone (PAEK) is a new type of thermoplastic resin with excellent comprehensive performance. It can withstand a continuous service temperature of 250 °C, which is significantly higher than that of traditional thermoplastic resin, and it still retains good mechanical properties at high temperature. At the same time, it has good compatibility with epoxy resin and other thermosetting resins, and it has good toughness and molding technology. In addition, PAEK materials show very good impact strength, high mechanical strength, good sliding and wear properties, and excellent chemical resistance. Previous studies indicated that PAEK/epoxy resin blends can form specific ductile microstructures and the toughness of materials was improved. Mechanical behaviors are well known to strongly affect the friction and wear performance [18–20]. Some studies focused on the nanomechanical behaviors and scratch damage in polymer composites at the nanoscale [1,21,22]. However, they mainly focused on the characterization of the topography and dimension of the fiber–matrix interface/interphase structure in fiber-reinforced resin matrix composites [23–25]. Kavouras et al. studied a commercial carbon fiber (CF)-reinforced epoxy matrix composite in order to study the induced damage mechanisms [23].

However, very few studies focused on the nanomechanical behaviors and tribological properties of bicomponent high-performance epoxy resin and various blends.

In our current work, the nanoindentation and nanoscratching properties of bicomponent epoxy resin blends were investigated. The effects of PAEK powders on the nanomechanical and tribological performance of the epoxy resin material were studied. The maximum load residual, residual indentation depth, microhardness, and modulus of elasticity can provide important information about the mechanical properties of the test materials. It is expected that this research will be helpful toward a

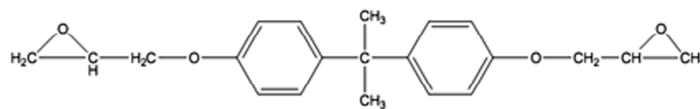
better understanding of the role of PAEK powders in the reinforcement of polymer composites on a nanoscale.

2. Experimental Details

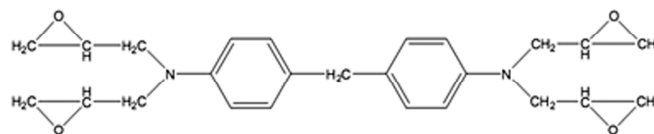
2.1. Raw Materials and Reagents

The diglycidyl ether of bisphenol A (DGEBA, E-54)-based epoxy resins were supplied by Wuxi Synthetic Resin (Jiangsu, P.R.C). *N,N,N',N'*-tetraglycidyl-4,4'-diaminodiphenylmethane (TGDDM, AG80) was provided by the Shanghai Synthetic Resins Research Institute (Shanghai, P.R.C). The curing agent diamino diphenyl sulfone (DDS) was supplied by Shanghai Reagent (Shanghai, P.R.C). The toughening agent was a modified polyaromatic ether ketone resin (PAEK) powder, which was provided by the Beijing Institute of Aeronautics Materials (Beijing, P.R.C). The chemical structures of the used compounds are shown in Figure 1.

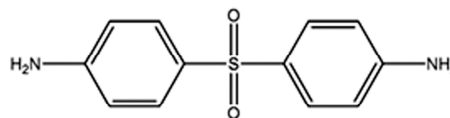
E54:



AG80:



DDS:



PAEK:

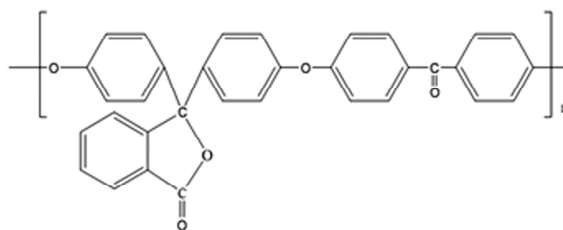


Figure 1. Structures of pristine epoxy resin, curing agent, and toughening agent.

2.2. Preparation of Epoxy Resin Casting Blends

Firstly, E-54 and AG80 resin were mixed at a proportion of 2:3, heating to a specified temperature. Then PAEK powders were added, and the mixture was stirred until completely dissolved and transparent. Finally, the curing agent (DDS powders) was added. The ratio of curing agent to E-54 resin was 1:1. The contents of PAEK powders with respect to epoxy precursors (mixture of epoxy monomer and hardener) were 10, 20, 30, and 40 phr (parts per hundred parts of resin). The above resins were mixed uniformly and poured into a metal mold. Subsequently, they were cured according to a

certain curing process for preparation of the resin casting body. Cured epoxy samples were recorded as BE, PAEK-10/BE, PAEK-20/BE, PAEK-30/BE, and PAEK-40/BE specimens, respectively.

2.3. Microstructure Characterization

The PAEK/BE blends were brittle fractured after being cooled in liquid nitrogen. Then, the fracture surfaces were coated with a thin layer of gold, and observed with an S-4800 scanning electron microscope (SEM) (Hitachi, Tokyo, Japan) at an accelerating voltage of 5 kV to characterize the two-phase structure of the blends.

2.4. Nanoindentation and Nanoscratch Tests

Both the nanoindentation and nanoscratch properties of the bicomponent epoxy resin and the composites were characterized by a Hysitron TriboIndenter[®] XP system (Hysitron, Eden Prairie, MN, USA). As the surface roughness significantly influences the attractive forces experienced by the indenter tip, prior to the experiment, each specimen was finely polished before the nanoindentation and nanoscratch experiments in order to produce the roughness. Then, the samples were cleaned with acetone-dipped cotton to remove surface contamination, followed by drying. In the nanoindentation test, the indented depth was recorded as a function of the applied force during a load/unload experiment. Nanoindentation was performed at the loading rate of $200 \mu\text{N}\cdot\text{s}^{-1}$ up to a peak load of $2000 \mu\text{N}$, where it was held for 10 s, and then unloaded completely at a negative rate of $200 \mu\text{N}\cdot\text{s}^{-1}$. Specifically, the loading, holding, and unloading times for nanoindentation were 10 s, 10 s, and 10 s, respectively. In this study, the indenter was a diamond pyramid, Berkovitch type, with a face angle of 142.35° . The most common values sought from nanoindentation testing with the TriboIndenter are sample hardness and elastic modulus. The hardness, elastic modulus, maximum indentation, and contact stiffness were also obtained from the curves using the Oliver and Pharr methods, and the results are listed in Table 1 [4]. Nanoscratching tests were performed following a ramp load procedure. They were conducted at a constant force of $500 \mu\text{N}$ and a total scratch length of $10 \mu\text{m}$. The scratch velocity was kept at $0.5 \mu\text{m}\cdot\text{s}^{-1}$ by controlling the X-Y stage movement. After the scratching was performed, the same tip was used to image the surface. The resultant scanning microscopy images were processed and evaluated using the image-processing software Hysitron TriboView. More than three nanoindentation or nanoscratch tests were performed for each sample in random locations to ensure reproducibility. The experiments were carried out at room temperature (25°C) and a relative humidity of 60%.

3. Results and Discussion

3.1. Microstructure Characterization

The fracture surface morphologies of the bicomponent epoxy resin and the composites are shown in Figure 2. It can be seen that many “wave-like” traces (arrowhead in Figure 2a), which are caused by rapid crack propagation, were produced on the fracture surface of the pure bicomponent epoxy resin. The fracture surface was relatively smooth and glassy, which indicated the typical brittle characteristic of highly cross-linked epoxy resin. In contrast, the micrographs obviously show that there was an increase in the fracture surface roughness of the various epoxy resins due to the addition of the PAEK powders, as shown in Figure 2b–f. This was due to the PAEK phase-separating and dispersing uniformly throughout the epoxy matrix in the process of solidification. An excellent interface connection between the dispersed phase PAEK particles and matrix was formed. Well-dispersed PAEK particles could cause crack initiation and termination under the action of stress. In Figure 2b, the continuous phase was epoxy and the thermoplastic (TP) resins were only dispersed in the epoxy continuum phase. An increase in the content of TP resins to 20 phr or higher led to a connected granular morphology, ascribed to a bicontinuous structure or phase-inverted structure. Figure 2c,d show the fracture surface morphologies of the BE/PAEK-20 sample. Note that the coexistence of

thermoplastic-coated thermosetting particles and a thermosetting resin-coated thermoplastic resin phase was generated (Figure 2c). However, at this moment, the thermoplastic-coated thermosetting particles were not continuous in the whole range; instead, it was a continuous trend, as shown in Figure 2d. Red lines and purple lines on the micrographs show the approximate boundaries of the phase and epoxy resin particles, respectively. The phase inversion was completed when the TP content was greater than or equal to 30 phr, as shown in Figure 2e,f. It can be seen that a connected granular morphology, ascribed to a bicontinuous structure and/or phase-inverted structure, was formed with the addition of TP fillers, as noted by Inoue [26]. The appearance of a thermoplastic resin coating the spherical thermosetting particles could happen in this case. In addition, the sizes of the spherical epoxy-rich phase domain tended to become smaller with the increase in thermoplastic resin content. At the same time, the particles squeezing each other became more and more irregular. This is consistent with the results reported in the literature [27].

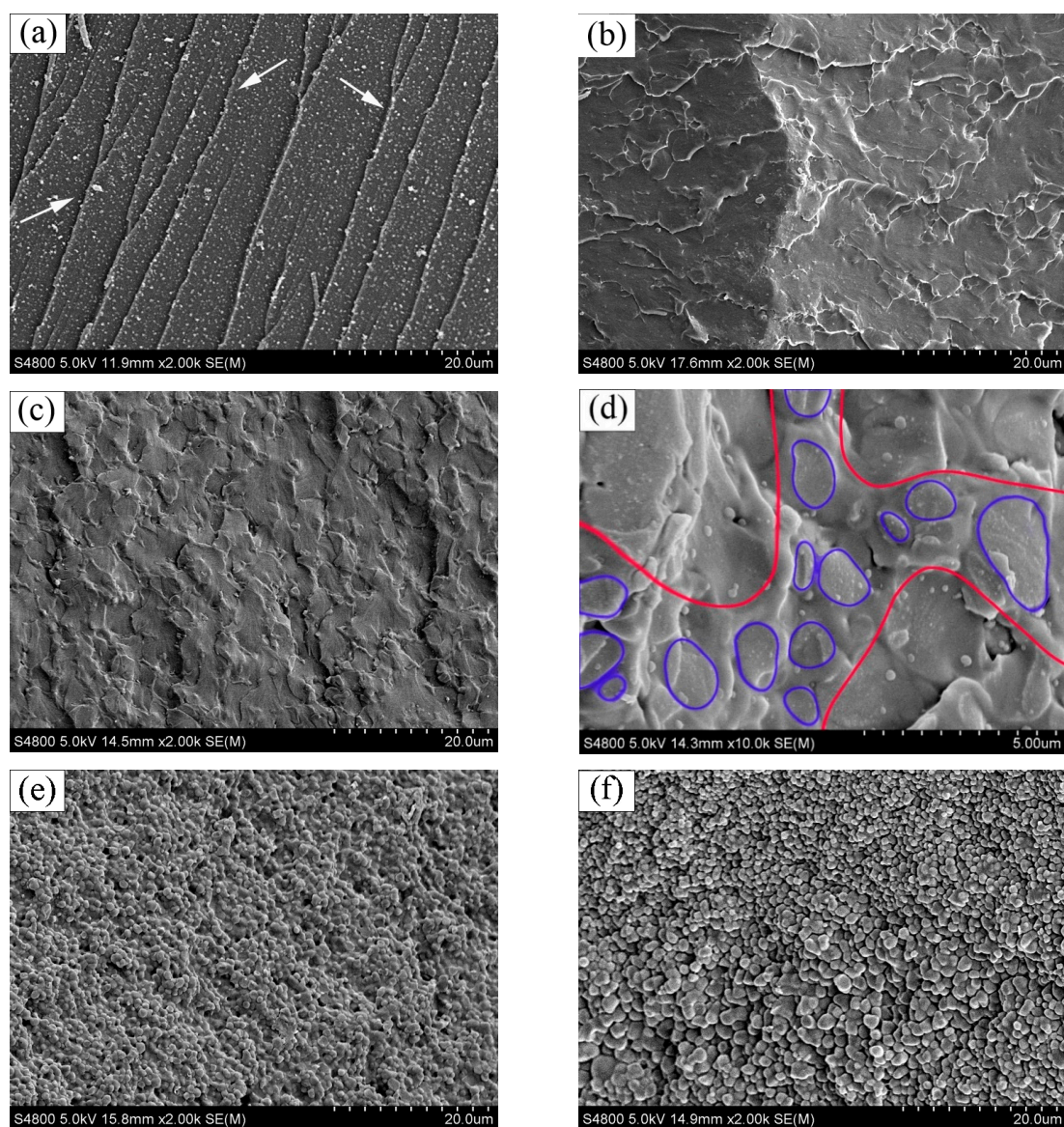


Figure 2. Morphologies of the impact fracture surfaces of bicomponent epoxy resin binary (BE) blends with polyaryletherketone (PAEK) powders: (a) pristine BE; (b) PAEK-10/BE; (c,d) PAEK-20/BE; (e) PAEK-30/BE; (f) PAEK-40/BE.

3.2. Nanoindentation Properties

Typical load vs. displacement curves of the bicomponent epoxy resin and the blends in the indentation test are shown in Figure 3. They exhibit the variations of the hardness and elastic modulus of the bicomponent epoxy resin and the composites. Clear differences in the depth of penetration among the five specimens can be seen. The loading part of the curves was a combination of elastic deformation and plastic deformation, while the unloading part was mainly dominated by the plastic deformation. This shows that the nanoindentation response was plasticity-dominated. The hardness and modulus of the samples are given in Table 1. The results clearly show that introducing PAEK powders into the bicomponent epoxy resin matrix contributed to decreases in the hardness, elastic modulus, and contact stiffness of the specimens. Similar observations were also reported in other polymer systems [28].

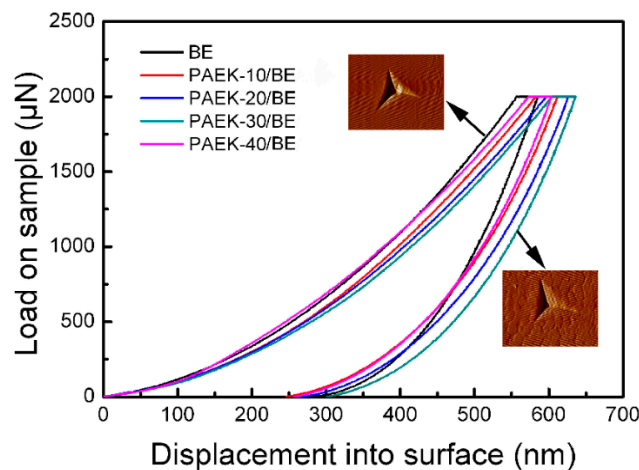


Figure 3. Typical load vs. displacement curves of the bicomponent high-performance epoxy resin and the composites.

As the content of PAEK powders approached 30 phr, the specimen's hardness properties decreased. In our previous work, we also found that for the content of PAEK powders up to 30 phr, the specimen had the highest fracture elongation under the same strain rate. It should be mentioned that granular structures in the SEM graphs also appeared, as shown in Figure 2d. This was very likely caused by the addition of the PAEK powders into the epoxy resin matrix. High-performance thermoplastics can significantly improve the toughness of epoxy resin and slightly reduce the hardness. The appearance of thermoplastic resin coating spherical thermosetting particles could happen when the content of PAEK powders was greater than or equal to 30 phr. In addition, the sizes of the spherical epoxy-rich phase domain tended to become smaller when the TP content was 40 phr, exhibiting higher hardness. The hardness exhibits the load-carrying capacity, and the elastic modulus represents the indentation recovery capacity. Higher values of hardness and elastic modulus mean a better load-carrying and indentation recovery capacity. Through a comparison of the five specimens, one can conclude that the neat bicomponent high-performance epoxy resin specimen has better load-carrying and indentation recovery capacity. This indicates that the bicomponent high-performance epoxy resin can provide excellent mechanical behaviors, such as high strength and fracture toughness [14]. As shown in Figure 3, the overall pattern in the load vs. displacement curves for the pristine bicomponent epoxy resin sample was similar to that of the composite specimens. It was noted that the incorporation of PAEK powders into the polymer matrix reduced the elastic modulus and slightly reduced the hardness. The elastic modulus reduced from 4.93 GPa for the neat bicomponent epoxy resin to 3.88 GPa for the PAEK-30/BE composite (about a 21.3% decrease). In addition, the hardness of the PAEK-30/BE composite samples decreased slightly compared to the pure bicomponent epoxy resin. In addition, a decrease of 13.3% in hardness from 302.54 MPa for the neat bicomponent epoxy resin to 262.25 MPa for the PAEK-30/BE composite was observed. As can be seen from Table 1, the maximum indentation

depths varied from 586.60 nm for the pristine bicomponent high-performance epoxy resin specimen to 635.37 nm for the PAEK-30/BE specimen. By increasing the PAEK powder content, the hardness and elastic modulus of the composites decreased, indicating an improvement in the plasticity index of the composites. The hardness of a material is defined as the degree of its resistance to plastic deformation [11,29]. Thus, the greater hardness of the neat bicomponent epoxy resin compared to the other samples contributed to the highest resistance to plastic deformation. At the loading stage, polymer chains in contact with PAEK powders have less time to recover elastically after removing the external load [21]. Therefore, more elastic deformations remain.

Table 1. Mechanical properties of the bicomponent epoxy resin (BE) and the composites with polyaryletherketone (PAEK) powders.

Specimen	Hardness	Elastic Modulus (GPa)	Maximum Indentation Depths (nm)	Contact Stiffness ($\mu\text{m}\cdot\text{nm}^{-1}$)
BE	302.54	4.93	586.60	14.30
PAEK-10/BE	292.48	3.99	615.27	11.88
PAEK-20/BE	281.35	3.90	626.41	11.75
PAEK-30/BE	262.25	3.88	635.37	11.73
PAEK-40/BE	298.56	4.08	603.62	12.92

3.3. Nanoscratch Properties

Nanoscratch experiments of the five samples were conducted at loads of 500 μN using the same Berkovich indenter as in the nanoindentation tests. In the nanoscratching tests, the indenter penetrates into the specimen matrix and slides along it. Therefore, frictional resistance between the indenter and specimen is inevitable. These parameters do not exist in the nanoindentation tests [22]. The lateral force as a function of the scratch distance and the scratch time under maximum normal loads for the bicomponent epoxy resin and the composites during the nanoscratch tests varied significantly, as shown in Figure 4a,b, respectively. Figure 4a depicts that the variation of the lateral force increased linearly as a function of the scratch distance of 10 nm. It is evident that the lateral force of the pristine bicomponent epoxy resin was highest, while that of the PAEK-30/BE binary blend was the lowest. The optical image of the pristine bicomponent epoxy resin in Figure 5a reveals that the nanoscratch morphology was broad and deep. The profile of the PAEK-30/BE specimen was the shallowest (Figure 5d). It can be also seen that the scratch broadened and deepened gradually with the increase in TP content.

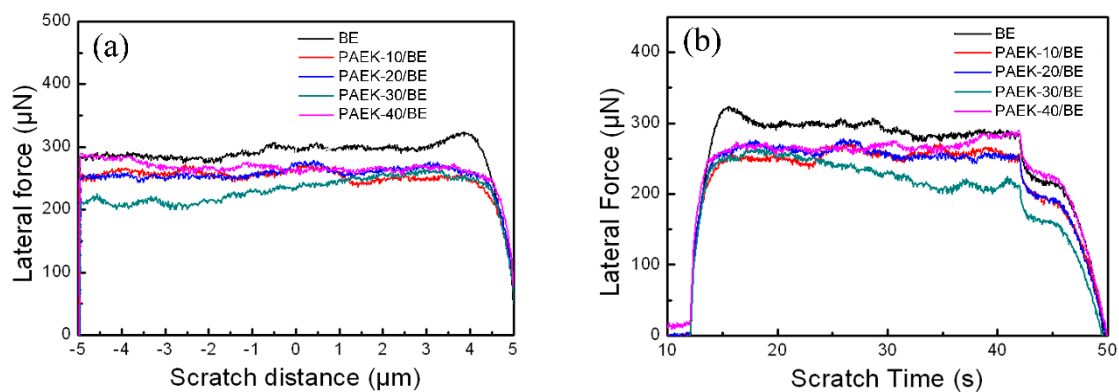


Figure 4. Variation of the lateral force as a function of (a) the scratch distance and (b) the scratch time under various maximum normal loads for the bicomponent epoxy resin and the blends.

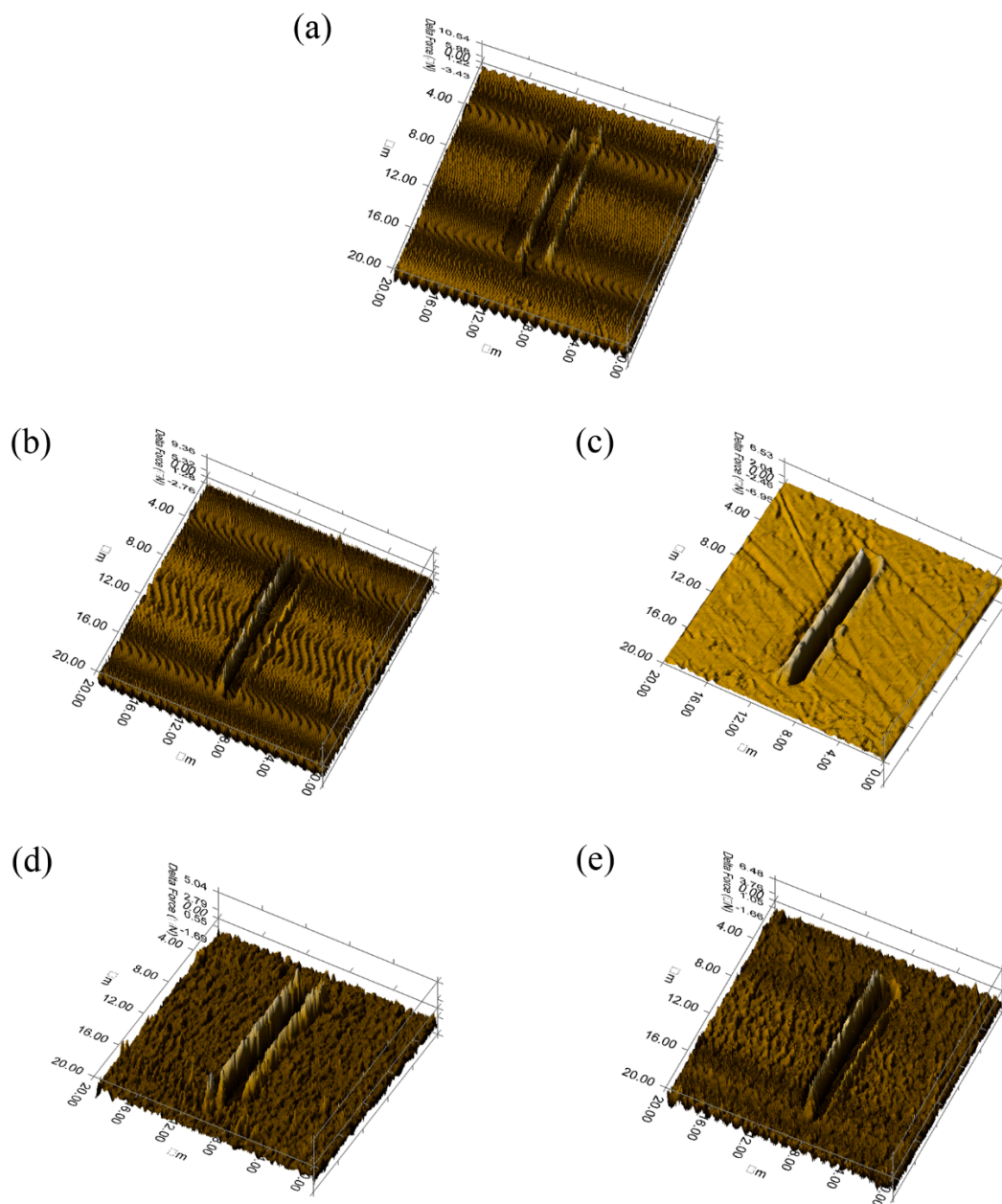


Figure 5. Scratch surface morphologies of the bicomponent epoxy resin and the blends with a $20 \times 20 \mu\text{m}$ field of view: (a) pristine BE; (b) PAEK-10/BE; (c) PAEK-20/BE; (d) PAEK-30/BE; (e) PAEK-40/BE.

Figure 5 shows the typical scratch surface morphology of the bicomponent epoxy resin and the blends. Three-dimensional (3D) micrographs showing differences in the nanoscratch behavior of the specimens at identical scratch conditions with a view field of $20 \times 20 \mu\text{m}$ are given in Figure 5. On the scratch tracks of all the samples, there were obvious pile-up materials on the walls of the groove. The shallowest groove was formed on the neat bicomponent epoxy resin matrix under the same nanoscratch conditions, and polymers plastically deformed if their surface ductility was higher. This is consistent with some previous research where it was found that, for superior nanoscratching resistance, polymers with higher modulus are preferred [8].

In Figure 6, the average coefficient of friction is plotted against the scratch time for the bicomponent epoxy resin and the composites at a load of $500 \mu\text{N}$ and a scratching speed of $0.5 \mu\text{m}\cdot\text{s}^{-1}$. It is evident in Figure 6 that the frictional coefficients were relatively low at the initial stage; then, they increased sharply with increasing sliding time and reach a steady state at a scratching duration of 15 s. Then,

the frictional coefficient decreased and then increased rapidly at 42 s. This was very likely caused by the variation in real contact area in the process of nanoscratch tests. According to Figure 6, the incorporation of PAEK powders into the bicomponent epoxy resin resulted in further enhancement of the mechanical properties. The steady-state frictional coefficient of the PAEK-30/BE binary blend was the smallest, while that of neat bicomponent epoxy resin was the highest. This indicated that the incorporation of thermoplastic PAEK powders was very effective in improving the scratch/wear resistance of the bicomponent epoxy resin.

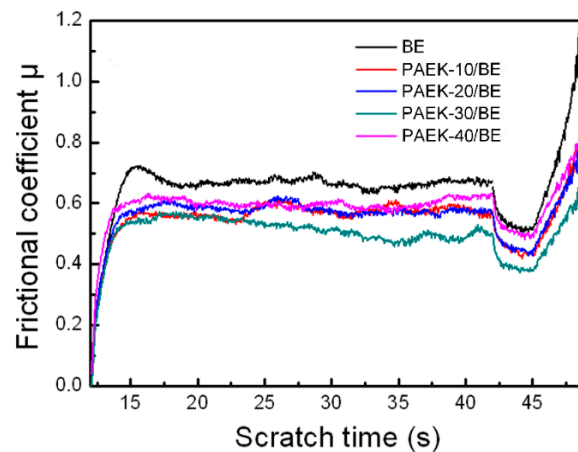


Figure 6. The coefficient of friction as a function of the scratch time for the bicomponent epoxy resin and the composites.

Figure 7 shows the variation of the normal depth along the scratch distance for the pure bicomponent epoxy resin and the PAEK-30/BE blend. In the PAEK-30/BE specimen, the tip pushed upward remarkably during the nanoscratching test, which indicated that this material was more resistant to scratching than the pristine bicomponent epoxy resin. This phenomenon indicates the effect of PAEK fillers on the scratch resistance of the composites. Figure 7 also shows the in situ nanoscratch images at the maximum load. It is clear that both surfaces were worn considerably under the same conditions. Plastic deformations and pile-up were observed for all specimens. The pile-up increased in size with the addition of PAEK powders.

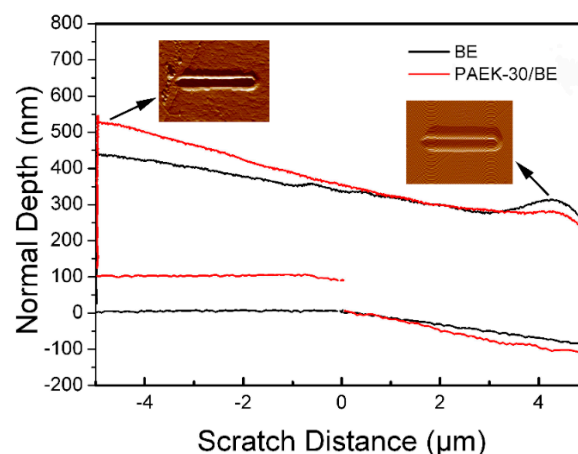


Figure 7. Variation of the normal depth along the scratch distance for the bicomponent epoxy resin and the composites.

4. Conclusions

Nanoindentation and nanoscratch testing revealed large differences in the mechanical properties of the bicomponent epoxy resin and the composites. The nanoindentation results indicated that the indentation response was a plasticity-dominated process. Through a comparison of the five samples, one can conclude that the pristine bicomponent epoxy resin has a better load-carrying and indentation recovery capacity. The hardness decreased as the content of PAEK powders approached 30 phr, while that of the neat bicomponent epoxy resin specimen was the highest. However, in the nanoscratch experiments, the frictional coefficient of the PAEK-30/BE blend was the lowest, while that of the pristine bicomponent epoxy resin was the highest. In other words, the PAEK-30/BE blend had the best scratch/wear resistance.

Author Contributions: Conceptualization, H.H and Z.L.; Methodology, H.H.; Software, Z.L.; Validation, H.H., Z.L. and C.W.; Formal analysis, L.M. and Y.S.; Investigation, C.W.; Data curation, Z.L.; Writing—original draft preparation, H.H., Z.L. and C.W.; Writing—review and editing, H.H., L.M.; Project administration, Z.L.

Funding: This work was supported by the National Natural Science Foundation of China (Grant No. 51605007) and the Anhui provincial Natural Science Foundation of China (No.1208085QB41). The authors would like to thank Xiaosu Yi and Ming Zhang of the National Key Laboratory of Advanced Composites in the Beijing Institute of Aeronautics Materials, who helped improve the quality of this paper.

Conflicts of Interest: The authors declare that no conflict of interest.

References

1. Dasari, A.; Yu, Z.Z.; Mai, Y.W. Nanoscratching of nylon 66-based ternary nanocomposites. *Acta Mater.* **2007**, *55*, 635–646. [[CrossRef](#)]
2. Wasmer, K.; Gassilloud, R.; Michler, J.; Ballif, C. Analysis of onset of dislocation nucleation during nanoindentation and nanoscratching of InP. *J. Mater. Res.* **2012**, *27*, 320–329. [[CrossRef](#)]
3. Saeed, Z.C.; Xu, S.Z. Nanoindentation/scratching at finite temperatures: Insights from atomistic-based modeling. *Prog. Mater. Sci.* **2019**, *100*, 1–20.
4. Liver, W.C.O.; Pharr, G.M. Improved technique for determining hardness and elastic-modulus using load and displacement sensing indentation experiments. *J. Mater. Res.* **1992**, *7*, 1564–1583.
5. Zhou, H.X.; Qiu, S.; Zhang, X.Z.; Xu, C. Mechanical characteristics of soft-brittle HgCdTe single crystals investigated using nanoindentation and nanoscratching. *Appl. Surf. Sci.* **2012**, *258*, 9756–9761. [[CrossRef](#)]
6. Gouldstone, A.; Chollacoop, N.; Dao, M.; Li, J.; Minor, A.M.; Shen, Y.L. Indentation across size scales and disciplines: Recent developments in experimentation and modelling. *Acta Mater.* **2007**, *55*, 4015–4039. [[CrossRef](#)]
7. Wong, M.; Lim, G.T.; Moyse, A.; Reddy, J.N.; Sue, H.J. A new test methodology for evaluating scratch resistance of polymers. *Wear* **2004**, *256*, 1214–1227. [[CrossRef](#)]
8. Wong, J.S.S.; Sue, H.J.; Zeng, K.Y.; Li, R.K.Y.; Mai, Y.W. Scratch damage of polymers in nanoscale. *Acta Mater.* **2004**, *52*, 431–443. [[CrossRef](#)]
9. Kim, J.K.; Hodzic, A. Nanoscale characterisation of thickness and properties of interphase in polymer matrix composites. *J. Adhesion* **2003**, *79*, 383–414. [[CrossRef](#)]
10. Carreon, A.H.; Funkenbusch, P.D. Material specific nanoscratch ploughing friction coefficient. *Tribol. Int.* **2018**, *126*, 363–375. [[CrossRef](#)]
11. Fischer-Cripps, A.C. *The IBIS Handbook of Nanoindentation*; Part 1; Fischer-Cripps Laboratories Pty Ltd.: Forestville, Australia, 2009.
12. Chiao, L. Mechanistic reaction kinetics of 4,4'-Diaminodiphenyl sulfone cured tetraglycidyl 4,4'-Diaminodiphenylmethane epoxy resins. *Macromolecules* **1990**, *23*, 1286–1290. [[CrossRef](#)]
13. Zhang, X.J.; Yi, X.S.; Xu, Y.Z. Cure-induced phase separation of Epoxy/DDS/PEK-C composites and its temperature dependency. *J. Appl. Polym. Sci.* **2008**, *109*, 2195–2206. [[CrossRef](#)]
14. Zhang, M.; An, X.F.; Tang, B.M.; Yi, X.S. TTT diagram and phase structure control of 2/4 functional epoxies blends used in advanced composites. *Front. Mater. Sci.* **2007**, *1*, 81–87. [[CrossRef](#)]
15. Xiang, C.; Sue, H.J.; Chu, J.; Coleman, B. Scratch behavior and material property relationship in polymers. *J. Polym. Sci. Part B Polym. Phys.* **2009**, *39*, 47–59. [[CrossRef](#)]

16. Yamanaka, K.; Ohmori, Y. Effect of boron on transformation of low-carbon low-alloy steels. *Trans. AIME* **1977**, *17*, 93–101.
17. Zamanian, M.; Mortezaei, M.; Salehnia, B.; Jam, J.E. Fracture toughness of epoxy polymer modified with nanosilica particles: Particle size effect. *Eng. Fract. Mech.* **2013**, *97*, 193–206. [[CrossRef](#)]
18. Leyland, A.; Matthews, A. On the significance of the H/E ratio in wear control: A nanocomposite approach to optimised tribological behaviour. *Wear* **2000**, *246*, 1–11. [[CrossRef](#)]
19. Gao, J.P.; Luedtke, W.D.; Landman, U. Nano-elastohydrodynamics-structure dynamics, and flow in nonuniform lubricated junctions. *Science* **1995**, *270*, 605–608. [[CrossRef](#)]
20. Riedo, E.; Brune, H. Young modulus dependence of nanoscopic coefficient in hard coatings. *Appl. Phys. Lett.* **2003**, *83*, 1986–1988. [[CrossRef](#)]
21. Shen, L.; Phang, I.Y.; Liu, T.; Zeng, K. Nanoindentation and morphological studies on nylon 66/organoclay nanocomposites. II. Effect of strain rate. *Polymer* **2004**, *45*, 8221–8229. [[CrossRef](#)]
22. Shokrieh, M.M.; Hosseinkhani, M.R.; Naimi-Jamal, M.R.; Tourani, H. Nanoindentation and nanoscratch investigations on graphene-based Nanocomposites. *Polym. Test.* **2013**, *32*, 45–51. [[CrossRef](#)]
23. Kavouras, P.; Dragatogiannis, D.A.; Batsouli, D.I.; Charitidis, C.A. Effect of local microstructure on the indentation induced damage of a fiber reinforced composite. *Polym. Test.* **2017**, *61*, 197–204. [[CrossRef](#)]
24. Tam, L.; Zhou, A.; Wu, C. Nanomechanical behavior of carbon fiber/epoxy interface in hygrothermal conditioning: A molecular dynamics study. *Mater. Today Commun.* **2019**, *19*, 495–505. [[CrossRef](#)]
25. Norambuena-Contreras, J.; Gonzalez-Torre, I.; Vivanco, J.F.; Gacitúa, W. Nanomechanical properties of polymeric fibres used in geosynthetics. *Polym. Test.* **2016**, *54*, 67–77. [[CrossRef](#)]
26. Inoue, T. Reaction-induced phase-decomposition in polymer blends. *Prog. Polym. Sci.* **1995**, *20*, 119–153. [[CrossRef](#)]
27. Kiefer, J.; Hiborn, J.G.; Hedrick, J.L. Chemically induced phase separation: A new technique for the synthesis of macroporous epoxy networks. *Polymer* **1996**, *37*, 5715–5725. [[CrossRef](#)]
28. Phang, I.Y.; Liu, T.X.; Mohamed, A. Morphology, thermal and mechanical properties of nylon 12/organoclay nanocomposites prepared by melt compounding. *Polym. Int.* **2005**, *54*, 456–464. [[CrossRef](#)]
29. Molazemhosseini, A.; Tourani, H.; Naimi-Jamal, M.R.; Khavandi, A. Nanoindentation and nanoscratching responses of PEEK based hybrid composites reinforced with short carbon fibers and nano-silica. *Polym. Test.* **2013**, *32*, 525–534. [[CrossRef](#)]



© 2019 by the authors. Licensee MDPI, Basel, Switzerland. This article is an open access article distributed under the terms and conditions of the Creative Commons Attribution (CC BY) license (<http://creativecommons.org/licenses/by/4.0/>).